Engineering Structures 33 (2011) 1052–1061

Contents lists available at ScienceDirect

Engineering Structures

journal homepage: www.elsevier.com/locate/engstruct

# Buckling restrained braces as structural fuses for the seismic retrofit of reinforced concrete bridge bents

Samer El-Bahey [a,*], Michel Bruneau [b]

[a] Stevenson & Associates, Inc. Phoenix, AZ, United States
[b] State University of New York at Buffalo, United States

ARTICLE INFO

*Article history:*
Received 30 October 2009
Received in revised form
9 December 2010
Accepted 10 December 2010
Available online 19 January 2011

*Keywords:*
Structural Fuses
Structural Design
Structural Steel
Seismic Analysis
Buckling Restrained Braces
Ductility

ABSTRACT

A structural fuse concept is proposed in which easily replaceable ductile structural steel elements are added to an RC bridge bent to increase its strength and stiffness, and also designed to sustain the seismic demand and dissipate all the seismic energy through hysteretic behavior of the fuses, while keeping the RC bridge piers elastic. While this concept could be implemented in both new and existing bridges, the focus here is on the retrofit of non-ductile reinforced concrete bridge bents. Several types of structural fuses can be used and implemented in bridges; the focus in this paper is on using Buckling Restrained Braces (BRB) for the retrofit of RC bridge bents. The results of a parametric formulation conducted introducing key parameters for the design procedure of the fuse system, validated by nonlinear time history analyses are presented. A proposed design procedure, using BRBs as metallic structural fuses, is found to be sufficiently reliable to design structural fuse systems with satisfactory seismic performance. A graphical representation to help find admissible solutions is used, and shows that the region of admissible solution decreases when the frame strength ratio increases as a larger fuse element is required to achieve an effective structural fuse concept.



## 1. Introduction

Providing reliable mechanisms for dissipation of the destructive earthquake energy is key for the safety of structures against intense earthquakes. Inelastic deformations can limit the forces in members allowing reasonable design dimensions; and provide hysteretic energy dissipation to the system. The concept of designing some sacrificial members, dissipating the seismic energy, while preserving the integrity of other main components is known as the structural fuse concept. The structural "ductile" fuse concept was first introduced by Roeder and Popov [1] for the eccentrically braced frame concept for steel frames, although at that time the fuses were defined as a capacity design concept, and they were not easily replaceable. Fintel and Ghosh [2] used a similar capacity design concept and designated plastic hinging of the beams to be structural fuses. Wada et al. [3] expanded on the structural fuse concept by defining "damage-controlled" or "damage tolerant" structures. The approach stated that the structure should have two separate components, the first being a moment frame designed to resist gravity loads only. The second is a system of passive energy dissipation elements designed to resist loads resulting from strong ground motions. The damage controlled structures concept was further investigated and improved following the 1995 Northridge and 1995 Hyogoken-Nabu earthquakes by Conner et al. [4], who used steel shear panels and Buckling Restrained Braces (BRBs). That study demonstrated that it was possible to control the seismic response of a building by adjusting the distribution of stiffness and hysteretic damping of the fuses. Further developments were proposed by Shimizu et al. [5], Takana et al. [6], Wada and Haung [7], Haung et al. [8]. In particular, Wada and Haung [9] implemented an approach based on the balance of energy to design tall building structures having either hysteretic dampers or viscous dampers. A comprehensive study of damage controlled structures was performed by Wada et al. [10] who presented its potential to design new constructions and retrofit existing structures. Vargas and Bruneau [11,12] studied the implementation of the structural fuse concept using metallic dampers to improve the structural behavior of systems under seismic loads. A systematic and simplified design procedure to achieve and implement a structural fuse concept that would limit damage to disposable structural elements for any general structure, without the need for complex analyses was introduced based on identifying regions of admissible solutions for the structural fuse concept using nonlinear time history analyses.

All the previous work on the structural fuse concept focused on implementations on buildings; while inelastic deformations have been relied upon to achieve ductile performance for bridges, a rigorous implementation of the complete structural fuse concept

* Corresponding author. Tel.: +1 716 471 1427.
*E-mail address:* selbahey@gmail.com (S. El-Bahey).

0141-0296/$ – see front matter © 2010 Elsevier Ltd. All rights reserved.
doi:10.1016/j.engstruct.2010.12.027

**Notations**

*The following symbols are used in this paper:*

| | |
|---|---|
| $A_b$ | BRB cross sectional area |
| $C_1$ | Modification factor to account for the influence of inelastic behavior on the response of the system |
| $c$ | Yielding ratio of the BRB |
| $D$ | Column diameter |
| $E_s$ | BRB elasticity modulus |
| $f_{yBRB}$ | BRB yield strength |
| $f_c^{/}$ | Concrete compressive strength |
| $H$ | Frame height |
| $K_{\text{eff}}$ | Elastic lateral stiffness of the bare frame |
| $K_b$ | Elastic lateral stiffness of the BRBs |
| $K_{\text{tot}}$ | Elastic lateral stiffness of the total system |
| $L_b$ | Total length of BRB |
| $L_{ysc}$ | Yielding length of BRB |
| $L$ | Frame width |
| $m$ | Mass of bent |
| $n$ | Number of BRBs |
| $R_d$ | Displacement magnification factor for short periods |
| $S_a$ | Spectral acceleration demand |
| $T_{\text{eff}}$ | Effective period of the total system |
| $T_s$ | Period at the end of constant design spectral acceleration plateau |
| $V_{yf}$ | Yield strength of the bare frame |
| $V_{yb}$ | Yield strength of the BRB |
| $V_{Df}$ | Maximum strength of the bare frame |
| $V_{y1}$ | Total system yield strength |
| $V_{y2}$ | Strength of the total system at the point of RC frame yielding |
| $V_p$ | Lateral strength of the total system at the onset of column failure |
| $V_e$ | Seismic demand on the total system if the system behaved elastically |
| $V_i$ | Shear strength of the frame columns |
| $V_n$ | Shear force consistent with the Load producing Flexure Failure of the frame columns |
| $\alpha$ | The ratio between the lateral stiffness of the BRB and the lateral stiffness of the bare frame |
| $\beta$ | Post-yield strain hardening stiffness ratio of the bare frame |
| $\theta$ | BRB angle |
| $\Delta_{yb}$ | BRB yield displacement |
| $\Delta_{yf}$ | Bare frame yield displacement |
| $\Delta_{Df}$ | Lateral displacement at the onset of bare frame damage |
| $\delta_t$ | Expected displacement after frame retrofit (also called target displacement) |
| $\varepsilon_b$ | BRB maximum strain demand |
| $\eta$ | BRB strength ratio |
| $\rho$ | Column reinforcement ratio |
| $\mu_{\max}$ | Maximum displacement ductility that the total system can withstand |
| $\mu_f$ | Bare frame displacement ductility |
| $\mu_b$ | BRB displacement ductility |
| $\mu_D$ | Is the maximum local member displacement ductility demand |
| $\xi$ | Frame strength ratio |

has not been used for bridges. This could be of benefit for both new and existing bridges. The retrofitting approach is attractive given that seismically deficient bridges remain in service. Recent earthquakes in the United States, Japan and several other countries have demonstrated this seismic vulnerability, particularly for reinforced concrete bridges. These vulnerabilities have varied from total collapse, such as in the 1995 Kobe earthquake [13], to minor cracking and concrete spalling, such as in the 2001 Nisqually earthquake [14]. A common problem for RC bridge piers designed prior to the 1970's is that they were not detailed to prevent shear failure due to seismic excitation, nor detailed for ductile flexural response. For example, 13 mm (No. 4) ties or hoops spaced at 300 mm were typically used irrespective of column size, longitudinal reinforcement, or seismic demands. Also, short lap splices were used in column hoops and ties; as a result, these would open-up after concrete cover spalling during a severe earthquake that brought these structures into the inelastic range.

In this paper, building on this previous work, applicability of the structural fuse design methodology is investigated from a bridge engineering context (i.e., accounting for the need to protect bridge piers susceptible to non-ductile shear failures, defining zones of admissible solutions without resorting to non-linear time-history analyses, and providing modification factors that account for the characteristics of design spectra in bridge specifications). The methodology is presented based on simple hypotheses related to the mechanics of parallel non-coupled structural systems and static equilibrium equations, in the perspective that specially detailed ductile structural steel elements are directly added to the bridge bent to increase its strength and stiffness while not effecting the original lateral behavior of the columns (i.e. non-coupled lateral systems). The structural fuses are also designed to sustain the seismic demand and dissipate all the seismic energy through hysteretic behavior of the fuses, while keeping the bridge piers elastic. The intent of this concept is to make the fuse replaceable while the gravity load resisting system remains in service. Although this replaceability feature was not explicitly verified experimentally in the current project, Vargas and Bruneau [11,12] accomplished it for other types of structures.

Although adding the fuses will apply axial forces (tension or compression) that could impact the strength of the columns at the plastic hinge locations, this impact was not included in the design procedure presented in this paper. For most bridge columns, the axial forces applied by the fuses will be a negligible percentage of the column axial capacity (particularly given that bridge columns generally have a large axial capacity in comparison to building columns), but for those instances when that would not be the case, the engineer can consider the modified column capacity as a simple additional verification step in the procedures presented here. The general concepts and procedures presented here can also accommodate more complex material behaviors if so desirable for final design. Several types of structural fuses can be used and implemented in bridges; the focus in this paper will be on using the BRBs as a structural fuse. While many types of BRBs have been proposed in the past, one type of commonly encountered BRBs consists of a steel core encased in a steel tube filled with concrete. The steel core carries the axial load while the outer tube, via the concrete provides lateral support to the core and prevents global buckling. Typically a thin layer of material along the steel core/concrete interface eliminates shear transfer during the elongation and contraction of the steel core and also accommodates its lateral expansion when in compression (other strategies also exist to achieve the same effect). This gives the steel core the ability to contract and elongate freely within the confining steel/concrete-tube assembly. A variety of these braces having various materials and geometries have been proposed and studied extensively over the last 10–15 years [15–23]. A summary of much of the early development of BRBs which use a steel core inside a concrete filled steel tube is provided in Fujimoto et al. [24].

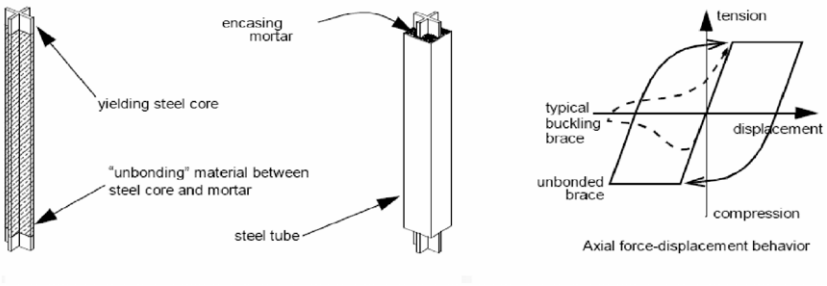


**Fig. 1.** Schematic mechanism of the BRB [23].

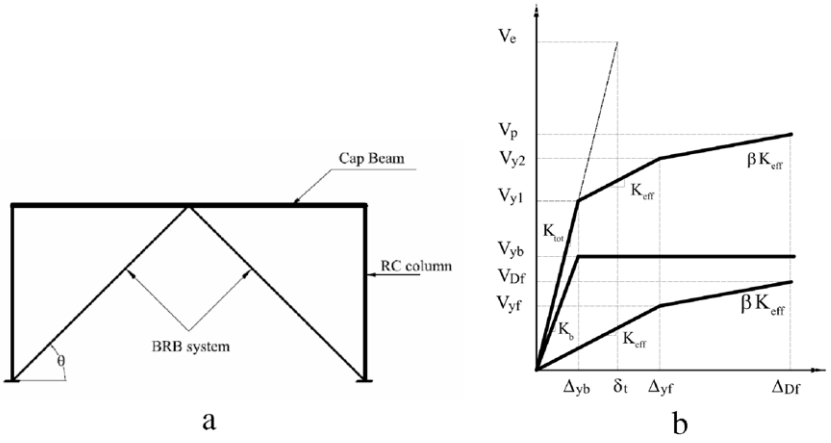


**Fig. 2.** (a) Layout of Studied Retrofit Scheme; (b) General Pushover curve.

The first tests in the United States were conducted in 1999 [25]. Fig. 1 shows a schematic mechanism of the BRB.

Results from a parametric study conducted to develop an understanding of the impact of various factors on helping to achieve the desired structural fuse behavior is presented, followed by a simplified design procedure to achieve and implement a structural fuse concept, validated by nonlinear time history analyses.

## 2. Parametric formulation

Fig. 2 schematically shows a simple two column RC bridge bent retrofitted using an inverted *V* (chevron) BRB system, a general pushover curve corresponding to this idealized structural system, and some of the important parameters used in this study. The bare frame and the BRBs are represented by bilinear models of respective $V_{yf}$ and $V_{yb}$, and the total curve is tri-linear with an initial lateral stiffness, $K_{\text{tot}}$, calculated by adding the effective lateral stiffness of the RC frame, $K_{\text{eff}}$, to the lateral stiffness of the BRB system, $K_b$.

For the structural fuse concept, it is required that the BRB yield displacement, $\Delta_{yb}$, be less that the yielding displacement of the frame, $\Delta_{yf}$. As a result, the BRB stiffness and strength must be chosen to limit the demand on the structure such that the system displacement reached for the maximum credible earthquake is less than $\Delta_{yf}$, concentrating energy dissipation in the BRB yielding, keeping the bare frame elastic. In this concept, the parameter represents the maximum displacement ductility that the system can withstand to ensure that the BRB acts as a structural fuse without yielding the RC bare frame, and is defined as:

$$\mu_{\max} = \frac{\Delta_{yf}}{\Delta_{yb}}. \tag{1}$$

Note that exceeding the $\mu_{\max}$ limit could occur for different reasons, mostly notably if the earthquake excitations in an actual event are stronger that the design earthquake, or for small bridge columns for which the axial forces coming from the fuses reduced their flexural strength if that flexure-axial interaction was accidentally not taken into account. However, again emphasizing that this is a fail-safe system, for ductile columns, the only problem that would occur is that after removal of the BRB, the yielded RC frame would not return to its original undamaged position.

In other instances though, yielding in the RC columns is not desirable and exceeding $\mu_{\max}$ could be more problematic. This could be the case in non-ductile bridge columns that either cannot sustain large plastic deformations to ensure energy dissipation, or that lack adequate transverse reinforcement and could suffer sudden shear failure.

In this perspective, $\mu_f$, is defined as the maximum displacement ductility that the frame can withstand, and is given by the ratio between the system displacement reached for the maximum credible earthquake (target displacement), $\delta_t$, and $\Delta_{yf}$.

$$\mu_f = \frac{\delta_t}{\Delta_{yf}}. \tag{2}$$

The BRB displacement ductility, $\mu_b$, is given by:

$$\mu_b = \frac{\delta_t}{\Delta_{yb}}. \tag{3}$$

It is effectively the global displacement ductility of the retrofitted structure, and should not exceed the maximum displacement ductility, $\mu_{\max}$, to meet the performance objectives.

The BRB maximum strain demand, $\varepsilon_b$, is a relation between $\delta_t$, the BRB total length, $L_b$, and the yielding ratio of the BRB, $c$, and the BRB angle, $\theta$, which can be written as

$$\varepsilon_b = \frac{\delta_t \cos\theta}{cL_b}. \tag{4}$$

Shear failure is a brittle failure mode that must also be considered. It can occur when inadequate transverse reinforcement is provided

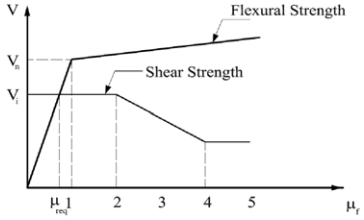


**Fig. 3.** Relation between shear and flexural failure.

such that shear failure would precede or prevent full development of ductile flexural hinging. To take into account the possibility of shear failure as a part of the structural fuse concept, the shear strength of the frame columns, $V_i$, must be compared to the shear force consistent with the Load producing Flexure Failure, $V_n$. Shear failure will occur if $V_i < V_n$, while flexural failure will occur if $V_i > V_n$; Fig. 3 schematically shows the relationship between shear and flexural failure for the first case. If brittle shear failure is the governing failure mode, then the limited displacement frame ductility at which the column remains elastic, $\mu_f$, (which would be less than 1 as illustrated in Fig. 3) is defined as:

$$\mu_f = \frac{V_i}{V_n}. \tag{5}$$

If $\delta_t$ is in the constant velocity region of the spectrum, it can be estimated using the equal displacement theory as:

$$\delta_t = \frac{V_e}{K_{\text{tot}}} \tag{6}$$

where $V_e$ is the elastic base shear, defined as the seismic demand on the total system if the system behaved elastically.

Three parameters are introduced to simplify the above equations, namely: the frame strength ratio, $\xi$, which relates the elastic base shear to the yield base shear of the bare frame; the stiffness ratio of the retrofitted frame, $\alpha$, which is the ratio between the lateral stiffness of the BRB and the lateral stiffness of the bare frame, and; the BRB strength ratio, $\eta$, which is the ratio between the elastic base shear and the yield base shear of the BRB.

$$\xi = \frac{V_e}{V_{yf}} \tag{7}$$

$$\alpha = \frac{K_b}{K_f} \tag{8}$$

$$\eta = \frac{V_e}{V_{yb}}. \tag{9}$$

Using these three new parameters, if the period lies in the constant velocity region of the spectra, $\mu_f$ and $\mu_b$ can be rewritten as:

$$\mu_f = \xi\left(\frac{1}{1+\alpha}\right) \tag{10}$$

$$\mu_b = \eta\left(\frac{\alpha}{1+\alpha}\right). \tag{11}$$

The maximum ductility can be expressed in terms of the new parameters as:

$$\mu_{\max} = \left(\frac{\eta}{\xi}\right)\alpha. \tag{12}$$

Shown in Fig. 4 are plots utilizing different values of $\xi$ considering steel grades A36 and A572 Gr.50. The horizontal axis is $\alpha$, while the vertical axis is $\mu_b$. Each solid line curve in the figure represents a constant value of $\eta$. The horizontal dashed lines correspond to specific values of $\mu_b$, which can be converted into equivalent BRB strains. The upper dashed horizontal line represents the BRB strain that is selected as the design limit (1.5% in this particular example). Although recent research have proven that a BRB could sustain cyclic plastic strains of up to 3% before fracture, this 1.5% limit was chosen as it is often cited in the literature as a common practical strain limit. The vertical dashed lines correspond to various values of $\mu_f$, obtained for specific values of $\alpha$, for a constant value $\xi$.

The region of admissible values of $\alpha$ and $\eta$ to achieve the structural fuse objectives is illustrated by the shaded area for a RC bridge bent having a typical flexural failure mode. The upper limit represents the maximum brace strain that can be achieved so that no fracture occurs in the brace, and the lower limit ($\mu_b = 1$) is the point below which the BRB will behave elastically and the benefits of having it dissipate energy will not exist. This region is vertically defined to the left by the value of $\mu_f$ corresponding to the applicable failure mode—here, $\mu_f = 1$ for flexural values, and lesser values if shear failures governed. The zone of admissible solution is unbounded to the right.

It can be seen that the region of admissible solutions decreases when increasing the values of $\xi$ and $f_{y\text{BRB}}$. This can be explained by considering that whenever the frame strength ratio increases, the strength of the bare frame decreases and, for a given stiffness ratio, $\alpha$, the value of the frame yield displacement will decrease followed by a decrease in the allowable ductility of the system, $\mu_{\max}$. Independently, increasing the value of BRB yield strength, $f_{y\text{BRB}}$, for a constant value of $\alpha$, increases the value of the BRB yield displacement, resulting in a reduction of the allowable ductility of the system and a proportional reduction in the value of $\mu_b$ when the strain limit of 1.5% is reached.

It can be seen that for a given value of stiffness ratio, increasing the BRB ductility would result in increasing the BRB strength ratio and accordingly decrease the BRB strength, which is expected because in order to increase the BRB ductility while preserving the stiffness, a reduction in the BRB strength is required in order to decrease the BRB yielding displacement and accordingly increase the BRB ductility. It can be seen that increasing the stiffness ratio corresponds to decreasing the frame stiffness, and for a given frame strength ratio, decreasing the frame stiffness would result in increasing the frame yielding displacement and also the frame ductility.

## 3. Modification factors

The previous plots were presented for cases for which the period was always considered to be in the constant velocity zone (i.e. $R_d = 1$ per AASHTO LRFD [26] or $C_1 = 1$ per NEHRP [27]). The correction factors are a period dependant parameter (i.e. depends on the mass and stiffness for each individual case). As a result, the transition point between the constant velocity and constant acceleration regions of the spectra is not tied to specific values of $\alpha$, which is why it was not considered in the previous plots. For design purposes, the effect of the correction factor should be calculated separately and used to magnify the BRB ductility and frame ductility values found from the above plots.

For example, the effect of adding the correction factor is illustrated for a RC bent configuration of mass equal to 33 kg s$^2$/mm, $\eta = 6$ and $\xi = 6$, in Figs. 5 and 6 which show the corrected BRB ductility and frame ductility values for different values of $\alpha$ respectively.

## 4. Nonlinear dynamic validation

To validate the above predicted system response based on pushover properties for retrofit using BRB structural fuses, a set of 9 artificial spectra-compatible accelerograms were generated using the TARSCTHS code [28]. The time histories matched the target acceleration response spectrum of the AASHTO LRFD.

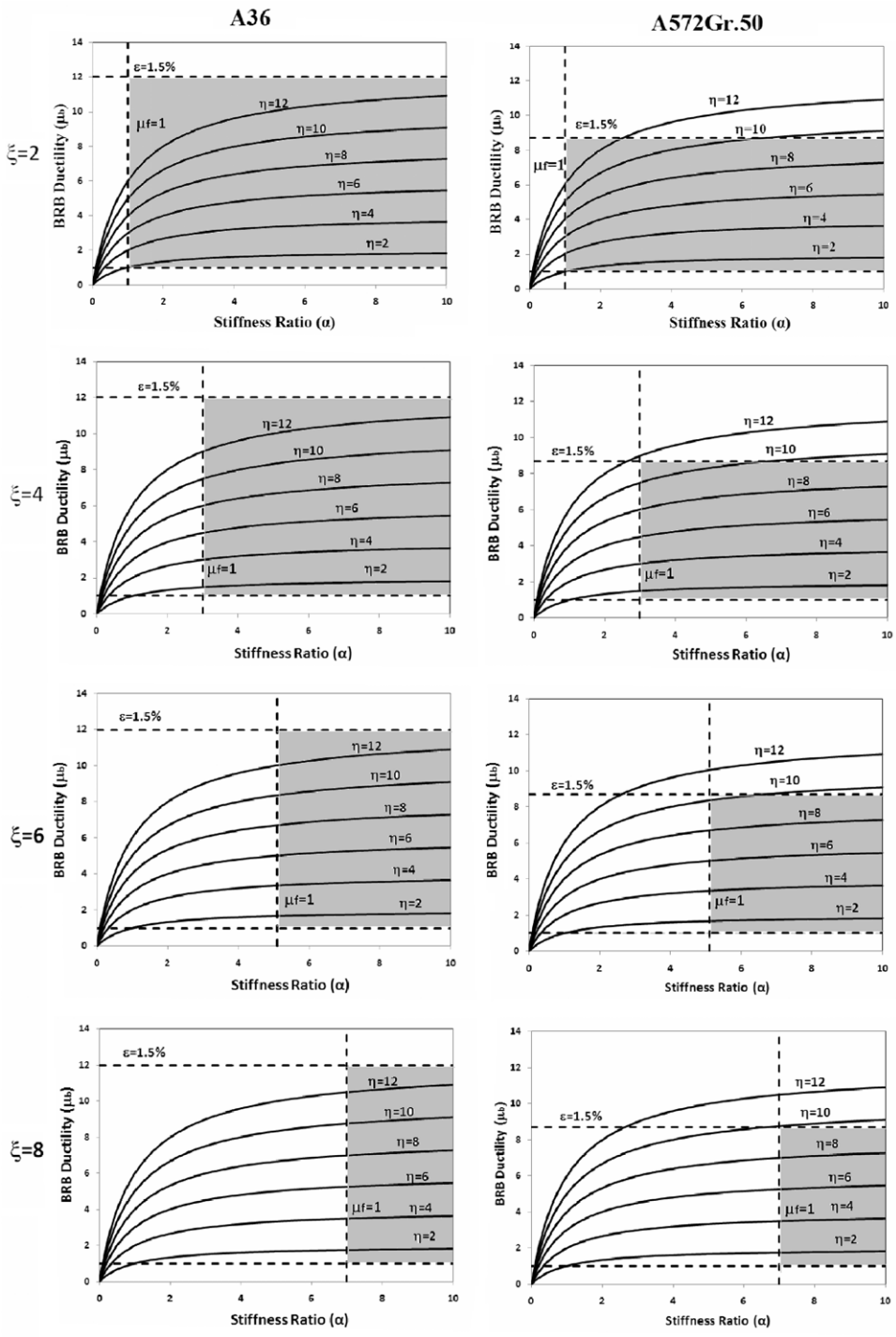


**Fig. 4.** Regions of admissible solutions for different $\xi$ (dimensionless parameter) and $f_{y_{BRB}}$.

Time history analysis was performed using the ABAQUS software [29] on a number of RC bents retrofitted by a chevron BRB bracing system configured. The total system mass was set to a constant value of 33 kg $s^2$/mm for all cases. Note that the chosen mass value was chosen as equal to that for a prototype bridge example presented in Priestley et al. [30].

A Bouc–Wen model [31] was chosen to represent the behavior of the BRBs which were modeled as truss elements. In particular, the model parameters (''*n*'', which is a dimensionless quantity that control the shape of the hysteretic loop, and the post-yield to elastic stiffness ratio ''*K*'') were assumed to have values equal to those usually suggested for BRBs [32,33] (i.e. $n = 1$, which implies a smooth transition from the elastic to the post-yielding regime, and $K = 0.025$).

A concrete damaged plasticity model [34,35] in ABAQUS was chosen to simulate the behavior of concrete. The model defined in ABAQUS is a continuum plasticity-based damage concrete model that assumes two main failure mechanisms; namely tensile cracking and compressive crushing of the concrete material, and for which the uni-axial tensile and compressive response of concrete is characterized by damaged plasticity. A typical A572 Gr.50 steel stress–strain curve was chosen to represent the re-bars and the BRB's yielding core material. The steel material nonlinearity was defined using the nonlinear

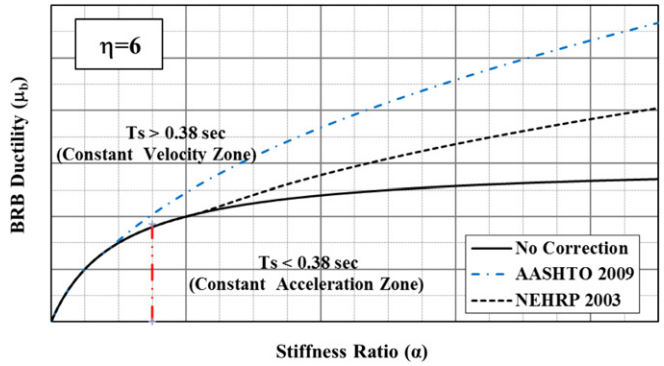


**Fig. 5.** Effect of adding the correction factors on the BRB ductility for $\eta = 6$ and $\xi = 6$.

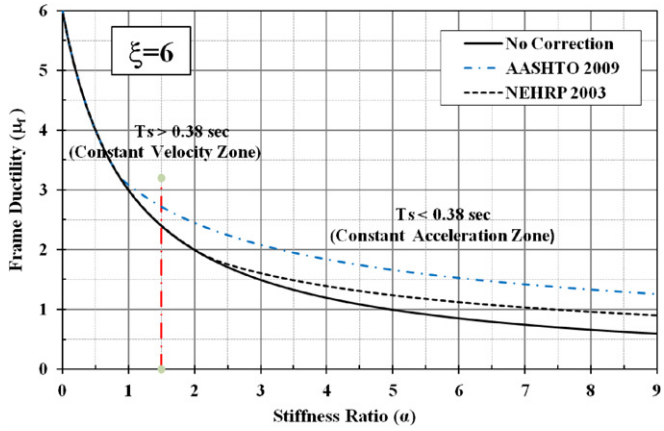


**Fig. 6.** Effect of adding the correction factors on the frame ductility for $\eta = 6$ and $\xi = 6$.

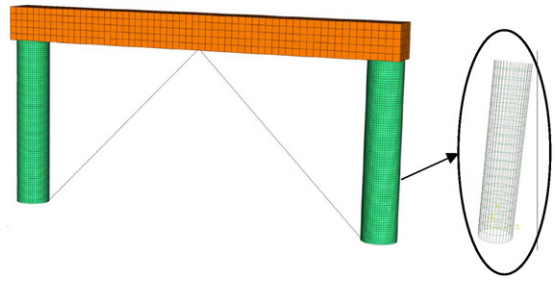

**Fig. 7.** Typical finite element model.

combined kinematic/isotropic hardening plasticity model. The re-bars' material nonlinearity was defined using the nonlinear combined kinematic/isotropic hardening plasticity model. C3D8R brick elements were used to model the concrete columns with embedded truss elements representing the re-bars and stirrups. Meshing of the concrete columns varied according to its dimensions. A typical finite element model is presented in Fig. 7 for a case with 1.25 m diameter columns with a 2% reinforcement ratio and typical 300 mm spacing stirrups. The height of the bent was equal to 6.25 m and span equal to 12.5 m and a 75 mm × 75 mm mesh. However, note that plastic behavior of the concrete is not significant here as the main intent is to keep the concrete columns in their elastic range.

Two sets of analyses were performed with a total of 72 time history analyses per set. For the first set of analyses, the values of $\xi$ and $\eta$ were chosen to be 2 for all cases. These values were chosen to ensure that all the system periods were in the constant

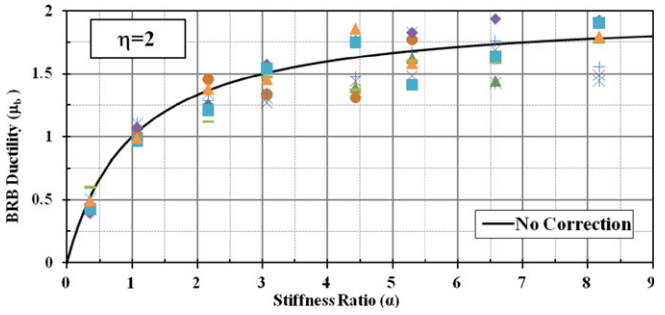


**Fig. 8.** Comparison between time history and push-over analysis results for BRB ductility at $\eta = 2$ and $\xi = 2$.

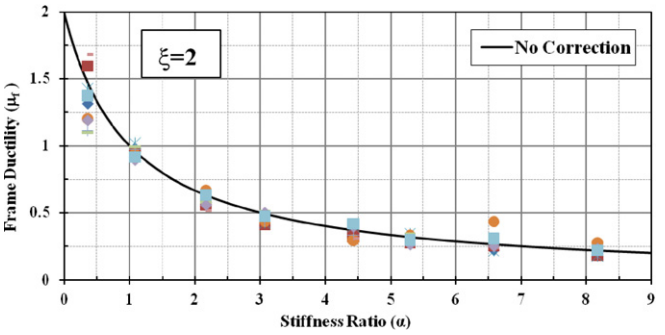


**Fig. 9.** Comparison between time history and push-over analysis results for frame ductility at $\eta = 2$ and $\xi = 2$.

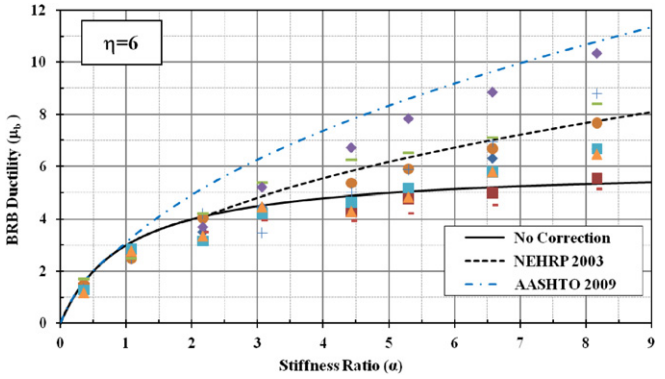


**Fig. 10.** Comparison between time history and push-over analysis results for BRB ductility at $\eta = 6$ and $\xi = 6$.

velocity zone of the spectra. Different values of $\alpha$ ranging between 1 and 8 were used and the corresponding values of frame and BRB ductilities were calculated and compared to those from the proposed static procedure. Figs. 8 and 9 show a comparison between the individual values obtained from all the synthetic records and the push-over analysis predictions for BRB and frame ductility respectively.

For the second set of analyses, the values of $\xi$ and $\eta$ was set to be equal to 6 for all cases. These values were chosen to show the effect of adding the correction factors for the cases in which the fundamental period of the total systems is in the constant acceleration zone of the spectra. Different values of $\alpha$ ranging between 1 and 8 were also used and the corresponding values of frame and BRB ductilities were calculated and compared to those from the push-over analysis predictions taking into account the correction factor. Figs. 10 and 11 show a comparison between the individual values obtained from all the synthetic records and the push-over analysis predictions for BRB and frame ductility

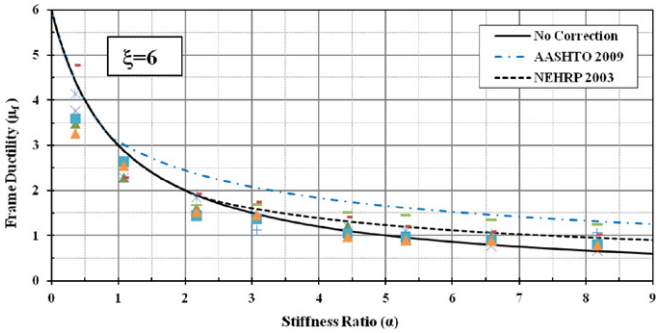


**Fig. 11.** Comparison between time history and push-over analysis results for frame ductility at $\eta = 6$ and $\xi = 6$.

respectively. Note that in those figures, the dotted lines correspond to the corrected values.

For both sets of analyses considered, the agreement is good between the response predicted by the simple procedure and the results from the non-linear time history analyses.

## 5. Retrofit design steps

The previous study conceptually showed that the structural fuse concept can be achieved for an RC bridge bent using a combination of different parameters. This knowledge must be augmented by guidelines on how to select suitable parameter values to achieve a satisfactory structural fuse system. For this purpose a retrofit procedure is proposed followed by a flow chart in Fig. 12 and consists of the following steps:

(1) Calculate the bare frame properties and perform a pushover analysis to define the idealized pushover curve from which $\Delta_{yf}$ and $V_{yf}$ can be obtained.
(2) Calculate initial shear strength of the bare frame $V_i$ using procedures from ACI 318 or from the procedure proposed by (Priestley et al.).
(3) Calculate the ratio $\frac{V_i}{V_{yf}}$.
(4) Establish the failure mode of the frame, if $\frac{V_i}{V_{yf}}$ is greater than 1, the frame will fail in flexure, and the desired $\mu_f$ is equal to 1. Otherwise, the frame will fail in shear and the desired $\mu_f$ is equal to the value of $\frac{V_i}{V_{yf}}$ (i.e. less than 1).
(5) Select a maximum permissible brace strain, $\varepsilon_b$, to comply with common design provisions for BRBs (a value of 1.5% is suggested).
(6) Calculate the effective period of the bare frame, which is used to obtain the spectral acceleration from the applicable response spectrum.
(7) Assume a spectral acceleration for the retrofitted frame. It should be greater than the one calculated for the bare frame, preferably assumed to be in the constant acceleration region of the spectrum to decrease the initial number of iterations.
(8) Estimate an initial value of $\xi$.
(9) Calculate the BRB angle according to the bent geometry. Using a chevron layout as

$$\theta = \tan^{-1}\left(\frac{2H}{L}\right). \tag{13}$$

(10) Calculate values of $\eta_{\max}$ and $\alpha_{\max}$ according to the calculated values of $\xi$ and $f_{y\mathrm{BRB}}$. These are the theoretical values for the maximum BRB strength required and the minimum stiffness ratio required to achieve the identified target ductilities. These values can be modified later if the calculated BRB area and strength are found to be impractical.
(11) Calculate the minimum required BRB stiffness and strength as:

$$K_{b_{\min}} = \alpha_{\min} K_f \tag{14}$$

$$V_{yb_{\min}} = \frac{S_a m}{\eta_{\max}} \tag{15}$$

from which the minimum required BRB area, $A_{b_{\min}}$, can be calculated as

$$A_{b_{\min}} = \frac{V_{yb_{\min}}}{2f_{y_{\mathrm{BRB}}}\cos\theta} \tag{16}$$

and the maximum yielding length of the BRB, $L_{\max}$, can be calculated as:

$$L_{\max} = \frac{2E_s A_{b_{\min}}\cos\theta}{K_{b_{\min}}}. \tag{17}$$

(12) Assess whether the area calculated above can be provided and accommodated by the system. If it is found to be excessive, another layout is to be selected while at the same time preserving the non-coupling assumption between the fuses and the columns individual lateral systems, and another angle, $\theta$, is recalculated. For the purpose of this study, if such is the case, an alternative BRB layout using multiple chevrons on top of each other is proposed—for common bridge columns sizes, the assumption of non-coupling between the bare bent and retrofitting fuses would remain true for this alternative layout, but final design checks would allow verifying this. For such a stacked chevron configuration, the new BRB angle, $\theta^*$, can be calculated as follows, based on the global geometry of the bent:

$$\theta^* = \tan^{-1}\left(\frac{2H}{nL}\right) \tag{18}$$

where $n$ is the number of chevron bracings.
The new BRB lateral stiffness to maintain the desired $\mu_f$ is calculated as:

$$K_b^{/} = \frac{n^2 E_s A_b^{/}\sin 2\theta^*}{\left(\frac{L_{ysc}}{L_b}\right)H} \tag{19}$$

while in case of a single chevron bracing system ($n = 2$) the BRB lateral stiffness is calculated as:

$$K_b = \frac{E_s A_b \sin 2\theta}{\left(\frac{L_{ysc}}{L_b}\right)H}. \tag{20}$$

It is required to maintain the same value of $\alpha$, from which the new lateral stiffness, $K_b^{/}$, must be equal to $K_b$, which leads to:

$$A_b^{/} = A_b\left(\frac{1}{n^2}\right)\left(\frac{\sin 2\theta}{\sin 2\theta^*}\right). \tag{21}$$

From which the number of BRBs, $n$, can be increased until a reasonable BRB area is achieved.
After calculating $A_b^{/}$, the corresponding maximum yielding BRB length, $L_{\max}^{/}$, is calculated as:

$$L_{\max}^{/} = \frac{2nE_s A_b^{/}\cos\theta^*}{K_b^{/}}. \tag{22}$$

(13) Determine if the calculated $L_{\max}^{/}$ is greater than the BRB cord length. If so, then this length can be reduced to the maximum practical length (i.e. 0.8 $L_b$) where $L_b$ is the BRB total length and the BRB area can be recalculated as:

$$A_b^{/} = \frac{0.8L_b K_b^{/}}{2nE_s\cos\theta^*}. \tag{23}$$

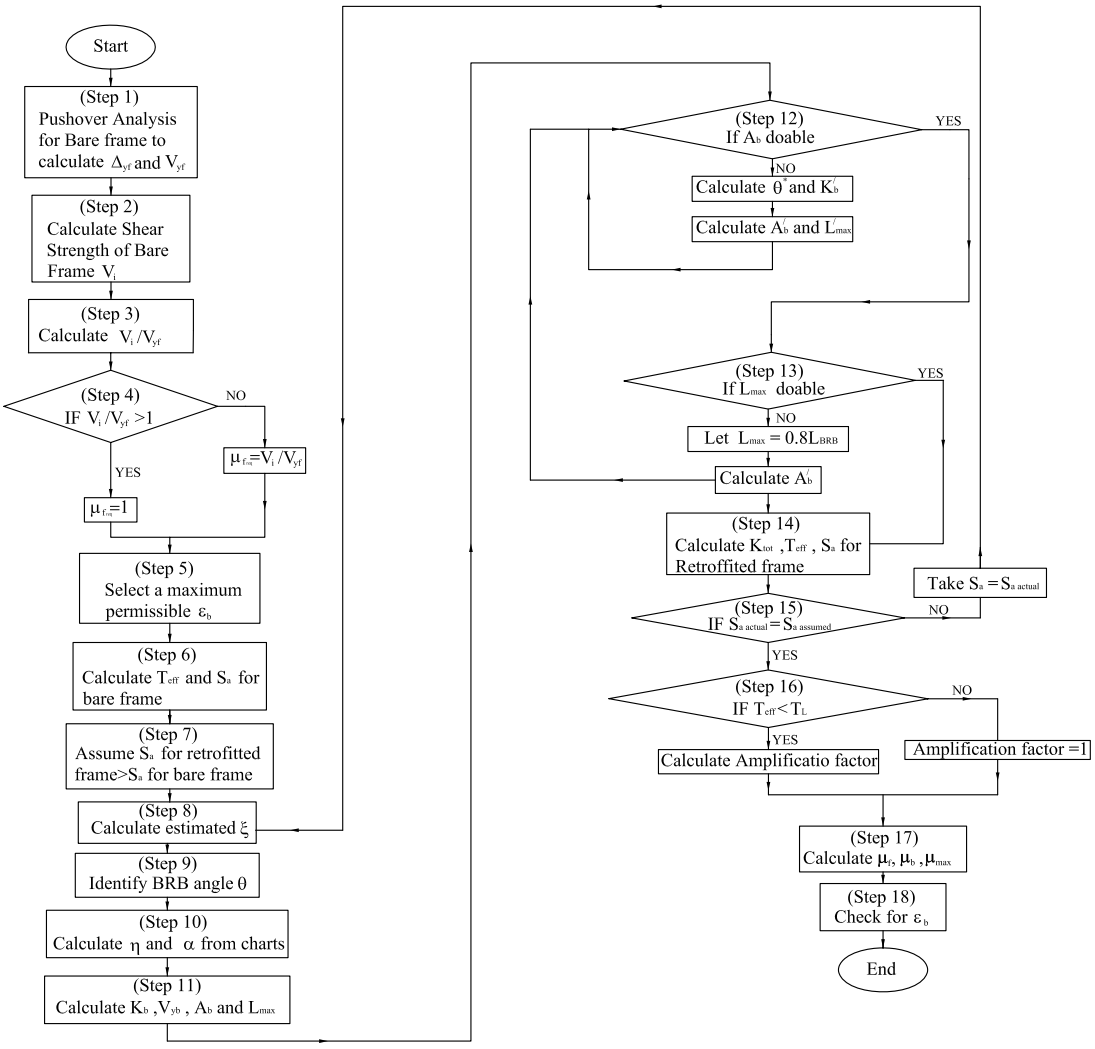


**Fig. 12.** Procedure to retrofit RC bridge bents satisfying the structural fuse concept.

Again if this area is impractical, step (11) is repeated until a reasonable value is obtained for $A_b^{/}$ and $L_{\max}^{/}$.

The value of $\eta^{/}$ is then calculated as

$$\eta^{/} = \eta \left(\frac{1}{n}\right)\left(\frac{A_b}{A_b^{/}}\right)\left(\frac{\cos\theta}{\cos\theta^{*}}\right). \tag{24}$$

(14) Calculate the total stiffness, the effective period of the retrofitted frame, and the actual spectral acceleration.

(15) Determine if the calculated spectral acceleration does not fall in the originally assumed "constant acceleration region". If so, then assume a new spectral acceleration and go to step (8) and iterate until $S_{a_{\text{assumed}}} = S_{a_{\text{actual}}}$.

(16) Calculate the values of $\mu_b$ and $\mu_f$, if the actual spectral acceleration lies in the constant acceleration zone, a modification must be applied to these values to take into account the equal energy theory as it was mentioned before that the charts was formed assuming the equal displacement theory. New values of $\mu_b$ and $\mu_f$ can be calculated as:

$$R_d = \left(1 - \frac{1}{\mu_D}\right)\frac{1.25T_s}{T_{\text{eff}}} + \frac{1}{\mu_D}. \tag{25}$$

(17) Recalculate the values of $\mu_f$ and $\mu_b$, and the value of $\mu_{\max}$, which would be equal to $\frac{\mu_b}{\mu_f}$.

(18) Check for BRB strain according to the following equation:

$$\varepsilon_b = \frac{f_{y_{\text{BRB}}}\mu_b}{E_s} \leq 1.5\%. \tag{26}$$

If not, go back to (step 12) and iterate.

## 6. Design example

An arbitrary RC bridge bent was selected with dimensions $L = 12\,700$ mm and $H = 6350$ mm. Columns were chosen to be circular with diameter $D = 1270$ mm having a longitudinal reinforcement ratio $\rho = 2\%$, and a transverse reinforcement similar to that of most bridges built prior 1970 (i.e. #4 bars spaced at 305 mm). Concrete strength, $f_c^{/}$, was assumed to be 4 kg/mm$^2$. The superstructure was assumed to be rigid so that the bent acted as a SDOF system with a lumped mass, $m$, of 33 kg s$^2$/mm acting at the top of the columns. A material strength, $f_{y\text{BRB}}$, of 28 kg/mm$^2$ was chosen for the BRBs. A response spectrum was constructed based on the AASHTO for LRFD for a site with soil-type class B. The site was chosen to represent an area exposed to severe ground shaking. A moment curvature analysis has been performed for the RC column and the calculated bare frame properties are: $V_{yf} = 307.3$ t, $\Delta_{yf} = 45$ mm, $K_{\text{eff}} = 4407$ t mm, $T_{\text{eff}} = 0.43$ s, $V_i = 529.3$ t (indicating that flexural yielding is dominating the response of the frame), and $\delta_t = 86$ mm (indicating that yielding

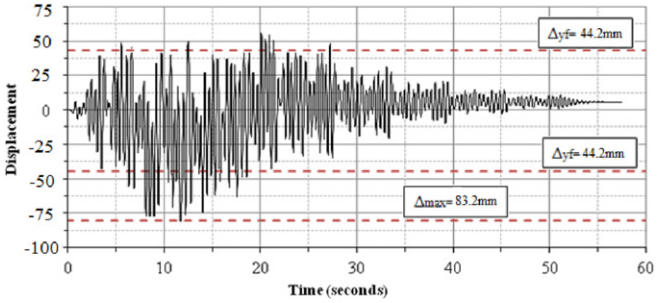


**Fig. 13.** Displacement time history plot of the bare frame.

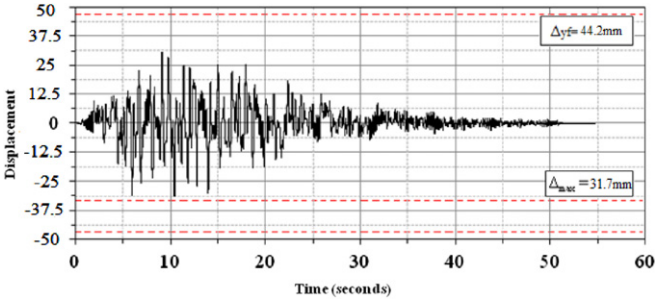


**Fig. 14.** Displacement time history plot of the retrofitted frame.

would occur in the columns) if the bare frame without BRBs was subjected to the design earthquake excitation. For the retrofitted system, a value of $\mu_f$ equal to 0.6 was assumed as a target parameter to account for the increase in ductility demand as the period of the retrofitted structure will most probably lie in the constant acceleration zone of the spectra. The BRB strength ratio, $\eta$, was taken equal to 6 to provide a reasonable BBR ductility ratio, $\mu_b$ of 4 and calculated using Eq. (3). The brace strain was limited to 1.5% for reasons described earlier. The frame strength ratio, $\xi$, was then calculated from Eq. (7) as 2.18, from which values of $\alpha = 2.5$ and $\eta = 6$ can be found from Eqs. (8) and (9) respectively. Assuming A572 Gr. 50 steel, $K_b$ and $V_{yb}$ were calculated from Eqs. (14) and (15) as 11 016 t mm, and 111.6 t respectively. $A_b$ and $L_b$ were then calculated from Eqs. (16) and (17) as 2865 mm$^2$, and 4750 mm respectively. Response parameters for the total system were then calculated as: $\Delta_{yb} = 6.6$ mm, $K_{\text{tot}} = 15\,151.5$ t mm, $T_{\text{eff}} = 0.23$ s, $R_d = 1.27$, $\delta_t = 35$ mm, $\varepsilon_b = 1.35\%$ (<1.5%). For comparison, one compliant ground record generated using the TARSCTHS code was chosen to illustrate typical time history results.

Displacement time history for the bare frame is shown in Fig. 13. It is observed that the bare frame undergoes inelastic deformations as the maximum displacement of 85 mm exceeds the frame yield displacement of 45 mm. Fig. 14 shows the displacement time history of the retrofitted frame, with a maximum displacement of 32 mm, which means that the columns remain elastic while the BRBs reach a ductility of 4.

## 7. Conclusions

This study specifically defines structural fuses as sacrificeable ductile structural elements designed to protect the columns of a bridge, allowing seismic energy dissipation by the fuses while the rest of the bridge substructure and superstructure remains elastic. Buckling restrained braces were proposed here as a structural fuse for retrofitting RC bridge bents to increase their strength and stiffness, and to dissipate seismic energy through hysteretic behavior while the bridge piers remain elastic. Governing parameters defining the behavior and design of the fuse system were identified. Seismic response was verified through parametric analyses of the studied systems and the results were refined and validated using non-linear time history analyses. Based on these results, a step-by-step design procedure for the seismic retrofit of RC bents using the fuse system was proposed. However, this methodology was based on the assumption that both the fuse and the column's lateral systems are non-coupled, and assuming that the axial forces from the fuses have a negligible impact on the column strength. Although each of these aspects can be accounted for using the presented methodology, as well as more complex material behaviors, applicability of these possible limitations must be assessed on a case-by-case basis.

The proposed procedure was found to be appropriate to design structural fuse systems with satisfactory seismic performance. It has been found that the range of admissible solutions that satisfy the structural fuse concept can be parametrically defined. From Fig. 4, it can be noted that the region of admissible solution decreases when the frame strength ratio increases as a larger fuse element will be required to achieve an effective structural fuse concept.

## 8. Future research needs

Experimental testing of bridge bents utilizing BRBs and other types of structural fuses should be conducted, followed by analytical work to verify and validate previous used numerical models. Improvements to the analytical models resulting from further validations are possible. Also a study on the effect of coupling both systems could be beneficial. The implementation of the structural fuse concept in bridge bents can also be expressed in many other creative ways that further research will help identify.

## Acknowledgements

This research was supported in part by the Federal Highway Administration under contract number DTFH61-07-C-00020 to the Multidisciplinary Center for Earthquake Engineering Research. However, any opinions, findings, conclusions and recommendations presented in this paper are those of the authors and do not necessarily reflect the views of the sponsors.

## References

[1] Roeder C, Popov E. Inelastic behavior of eccentric braced steel frames under cyclic loadings. Report no. 77. vol. 18. Berkeley: Earthquake Engineering Research Center, University of California; 1977.
[2] Fintel M, Ghosh S. Structural fuse: an inelastic approach to seismic design of buildings. Civil Eng, ASCE 1981;51:48–51.
[3] Wada A. et al. Damage tolerant structures. In: Proceedings of: fifth US–Japan workshop on the improvement of structural design and construction practices. Applied Council Technology. 1994. p. 27–39.
[4] Fellow J, et al. Damage-controlled structures. I: preliminary design methodology for seismically active regions. J Struct Eng 1997;123:423.
[5] Shimizu K, et al. Application of damage control structure using energy absorption panel. Struct Eng World Wide 1998; Elsevier Science, Ltd.
[6] Tanaka K, et al. Practical application of damage tolerant structures with seismic control panel using low-yield-point-steel to a high-rise steel building. Struct Eng World Wide 1998.
[7] Wada A, Huang Y. Damage-controlled structures in Japan. In: US–Japan workshop on performance-based earthquake engineering methodology for reinforced concrete building structures. 1999. p. 279–89.
[8] Huang Y, et al. Design of damage-controlled structures. In: Innovative approaches to earthquake engineering. Billerica (MA): WIT Press; 2002. p. 85–118.
[9] Wada A, Huang Y. Preliminary seismic design of damage tolerant tall building structures. In: Proceedings of symposium on a new direction in seismic design. Architectural Institute of Japan. 1995. p. 77–93.
[10] Wada A, et al. Passive damping technology for buildings in Japan. Prog Struct Eng Mater 2000;2.
[11] Vargas R, Bruneau M. Analytical response and design of buildings with metallic structural fuses. I. J Struct Eng 2009;135:386.
[12] Vargas R, Bruneau M. Experimental response of buildings designed with metallic structural fuses. II. J Struct Eng 2009;135:394.

[13] Schiff A. Hyogoken–Nanbu (Kobe) earthquake of January 17, 1995: lifeline performance. Amer Society of Civil Engineers; 1998.
[14] Ranf R, et al. Post-earthquake prioritization of bridge inspections. Earthq Spectra 2007;23:131.
[15] Saeki E, et al. Experimental study on practical-scale unbonded braces. J Struct Constr Eng AIJ 1995;476:149–58.
[16] Hasegawa H, et al. Experimental study on dynamic behavior of unbonded braces. J Arch 1999;114:103–6.
[17] Iwata M, et al. Buckling-restrained braces as hysteretic dampers. In: STESSA. Rotterdam: Balkema; 2000. p. 33.
[18] Black C, et al. Component testing, stability analysis and characterization of buckling-restrained unbonded braces. Pacific Earthquake Engineering Research Center; 2002.
[19] López W, et al. Lessons learned from large-scale tests of unbonded braced frame subassemblages. In: Proceedings, 71st annual convention, structural engineers association of california; 2002. p. 171–83.
[20] Sabelli R, et al. Seismic demands on steel braced frame buildings with buckling-restrained braces. Eng Struct 2003;25:655–66.
[21] López W, Sabelli R. Seismic design of buckling-restrained braced frames. Steel Tips, Structural Steel Education Council. 2004. www.steeltips.org.
[22] Iwata M, Murai M. Buckling-restrained brace using steel mortar planks; performance evaluation as a hysteretic damper. Earthq Eng Struct Dyn 2006; 35:1807–26.
[23] Clark P, et al. Large-scale testing of steel unbonded braces for energy dissipation. In: Advanced technology in structural engineering: proc., 2000 structures congress. Reston, VA: ASCE; 2000.
[24] Fujimoto M, et al. A study on the unbonded brace encased in buckling-restraining concrete and steel tube. J Struct Constr Eng, AIJ 1988;34:249–58.
[25] Aiken I, et al. Large-scale testing of buckling restrained braced frames. In: Proceedings, Japan passive control symposium. Japan: Tokyo Institute of Technology; 2002. p. 35–44.
[26] Aashto L. Bridge design specifications, customary US units, with 2009 interim revisions. Washington (DC): American Association of State Highway and Transportation Officials; 2009.
[27] BSSC NEHRP recommended provisions for seismic regulations for new buildings and other structures. Report no. FEMA 368. Building Seismic Safety Council; 2003.
[28] Papageorgiou A. et al. TARSCTHS, a computer program for target acceleration spectra compatible time histories. New York: Department of Civil, Structural and Environmental Engineering, University at Buffalo; 2001.
[29] ABAQUS, I. "ABAQUS/CAE user's manual." Electronic version, 6. 2005. p. 4–5.
[30] Priestley M, Seible F, Calvi G. Seismic design and retrofit of bridges. Wiley-Interscience; 1996.
[31] Wen Y. Method for random vibration of hysteretic systems. J Eng Mech Div 1976;102(2):249–63.
[32] Black C, Makris N, Aiken I. Component testing, stability analysis and characterization of buckling restrained braces. PEER report 2002/08. Pacific Earthquake Engineering Research Center, University of California at Berkeley; 2002.
[33] Tsai KC, Lai JW, Hwang YC, Lin SL, Weng YT. Research and application of double-core buckling restrained braces in Taiwan. In: Proceedings of the 13th world conference on earthquake engineering. 2004.
[34] Lee J, Fenves GL. Plastic-damage model for cyclic loading of concrete structures. J Eng Mech 1998;124:892.
[35] Lubliner J, Oliver J, Oller S, Onate E. A plastic-damage model for concrete. Internat J Solids Struct 1989;25(3):299–326.